http://dx.doi.org/10.5012/bkcs.2014.35.10.2979

Synthesis of Silver-doped Silica-complex Nanoparticles for Antibacterial Materials

Yu-Shik Shin, Mira Park, Hak-Yong Kim,[*] Fan-Long Jin,[†,‡] and Soo-Jin Park[‡,*]

Department of BIN Fusion Technology, Chonbuk National University, Chonju 561-756, Korea. [*]E-mail: khy@jbnu.ac.kr
[†]Department of Polymer Materials, Jilin Institute of Chemical Technology, Jilin City 132022, People's Republic of China
[‡]Department of Chemistry, Inha University, Incheon 402-751, Korea. [*]E-mail: sjpark@inha.ac.kr
Received May 9, 2014, Accepted June 13, 2014

Silver nanoparticles have been synthesized by liquid-phase and alcohol reduction methods. Silver-doped silica-complex nanoparticles were prepared using a sol–gel process. The formation, structure, morphology, and particle size of the nanoparticles have been studied using several techniques. Silver nanoparticles of size of 30-40 nm were formed successfully by alcohol reduction. TEM images show that both the concentration and the molecular weight of polyvinyl pyrrolidone (PVP) considerably affect the size of the emerging silver nanoparticles. The number of silver-doped silica-complex particles increased by a mercapto-group treatment that showed a narrower size distribution than that of silica treated with amino groups. The silver/polyester and silver-doped silica/polyester masterbatch chips showed excellent antibacterial activity against *Staphylococcus aureus* and *Escherichia coli*.

Key Words : Silver, Nanoparticles, Silica, Particle size, Antimicrobial activity

Introduction

Silver has high malleability, ductility, electrical and thermal conductivity, and good oxidation resistance at high temperature. These properties are widely used in industrial and consumer products.[1-3] Before antibiotics were invented, silver particles were used for injury and bacteria-infection treatments, as well as to protect humans from hospital bacteria because metallic silver particles have antibiotic and sterilizing effects against various bacteria.[4-6]

After the emergence of nanotechnology, metallic nanoparticles can be prepared and their physical, chemical, and optical properties were improved significantly. When the appearance of silver was changed to silver nanoparticles, the sterilizing effect against bacteria was increased significantly. This characteristic can be applied to existing products that are made of human-friendly materials.[7,8]

Silver nanoparticles can be synthesized by physical, chemical, and biological methods.[9,10] Synthesis and application of silver nanoparticles have been studied by several researchers. El-Rafie *et al.* synthesized silver-nanoparticle solutions using a fungi-based technique.[11] The obtained solutions exhibited silver-nanoparticle concentrations of about 2160 ppm with an average size in the range of 3-8 nm. Tang *et al.* prepared green, blue, red, and yellow silver nanoparticles by the photoinducing method.[12] The shapes of the obtained silver nanoparticles were prisms, spheres, and disks. Yang *et al.* synthesized silver nanoparticles using a biological route in which the pH, mango-peel extract content, silver-salt concentration, and incubation temperature are important parameters for controlling the size of the silver nanoparticles.[9] Montazer *et al.* prepared silver nanoparticles by UV irradiation.[13] The bacteria reduction ratio of fabrics treated with silver nanoparticles at a concentration of 200 ppm was more than 99% against *Staphylococcus aureus* (*S. aureus*, gram-positive bacteria) and *Escherichia coli* (*E. coli*, gram-negative bacteria). Tarimala *et al.* prepared a sol of silver-nanoparticle doped silica using a sol-gel process.[14] Woven cotton fabrics treated with this silica sol showed excellent antibacterial performance against *E. coli*.

In this study, silver nanoparticles were prepared by liquid-phase and alcohol reduction, and silver-doped silica-complex nanoparticles were prepared using a sol–gel process. The polyester masterbatch chip was coated with these nanoparticles in order to induce an antibacterial property.

Experimental

Materials. Silver nitrate, ferrous sulfate dihydrate, sodium citrate dihydrate, and hydrazine were purchased from Kojima Chemical Co., Ltd. Polyoxyethylene (20)sorbitan monolaurate (Tween 20), 3-aminopropyl trimethoxy silane (APTMS), and mercaptopropyl trimethoxy silane (MPTMS) were supplied by Daejung Chemicals & Metal Co., Ltd. A series of polyvinyl pyrrolidone (PVP) was purchased from International Specialty Products. Ethanol was supplied by Kojima Chemical Co., Ltd.

Synthesis of Silver Nanoparticles. (1) Liquid-phase reduction: Silver nitrate (0.1 mol, 16.99 g) was dissolved in distilled water (100 mL), and the temperature of the solution was controlled to be below 10 °C. Ferrous sulfate dihydrate (0.01 mol, 2.78 g) and sodium citrate dihydrate (0.1 mol, 29.41 g) was dissolved in distilled water (100 mL) and the solution added to the silver nitrate solution. After the reaction, the solution was centrifugally separated to removal unreacted material. The obtained cake was treated with sodium citrate dihydrate solution and washed with acetone several times. Finally, silver nanoparticles were obtained.

(2) Alcohol reduction: Silver nitrate (0.1 mol, 16.99 g) was dispersed in ethanol (100 mL), and the solution was heated under reflux. The silver ions were reduced to silver atoms according to the redox reaction, and the reduced silver atoms form silver particles by the growth and stabilization of nuclei, as shown in Figure 1. If an appropriate polymer, such as PVP was added and the above-mentioned reaction was carried out, the polymer acts as a dispersant and, thus, silver nanoparticles or silver-nanoparticle colloids are obtained. The molar ratio of polymer/silver nitrate was 0.5-2.

Preparation of Silver-doped Silica-complex Nanoparticles. Silica (size: 50-80 nm) was added to ethanol and stirred for 1 h. Amino-group containing APTMS or mercapto-group containing MPTMS was added to the solution. The solution was sonicated for 5 min and stirred for 6 h at room temperature. The solution was centrifugally separated and washed with ethanol three times. The obtained silica slurry was dissolved in distilled water. Silver salt was added to the solution and refluxed for 10 h. Finally, silver-doped silica-complex nanoparticles were obtained.

Preparation of Masterbatch Chips. Silver nanoparticles, silver-doped silica-complex nanoparticles, and a polyester chip were dried at 80 °C under vacuum and mixed at 150 °C for 10 min using a mixing mill. The silver content of the silver-doped silica-complex nanoparticles was 0.3 wt %.

Characterization and Measurements. The surface morphology of the silver nanoparticles was investigated using a scanning electron microscope (SEM, JEOL JXA840A).

The structure and crystallinity of the silver nanoparticles was investigated using X-ray diffraction (XRD, Rint-2000, Rigaku).

The formation process of the silver nanoparticles was investigated using a UV-vis spectrophotometer (UV-1650PC double-beam spectrophotometer, Shimadzu).

The surface morphology, particle size, and particle distribution of silver nanoparticles was investigated using field-emission scanning transmission electron microscopy (TEM, JEOL, JSM-6330F).

The masterbatch chip was treated by acidic hydrolysis and, then, the silver content of the chip was measured using inductively coupled plasma atomic emission spectroscopy (ICP-AES, PerkinElmer, Optima 4300DV).

The antimicrobial properties of the chip were examined according to the KSK 0693-test method against *E. coli* and *S. aureus*. A liquid cell culture was prepared, divided into two flasks, and sterilized. The two bacterial species were added and the solutions were cultivated at 37 °C for 24 h. The cultivated Gram's solution was diluted by a sterilized physiological salt solution. A solid cell culture was prepared and Gram's solution was inoculated with the culture. The culture was cultivated at 37 °C for 24 h, and the bacterial reduction ratio was calculated using the following equation:

$$R(\%) = \frac{(M_a - M_b)}{M_a} \times 100 \quad (1)$$

there R is the bacterial reduction ratio, M_a is the initial number of bacteria, and M_b is the number of bacteria after inoculation of microorganism.

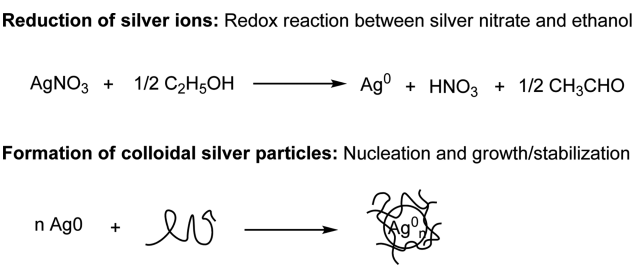

Figure 1. Preparation method of metal nanoparticles using alcohol-reduction method.

Results and Discussion

Properties of Silver Nanoparticles. Table 1 shows the particle size and morphology of silver nanoparticles prepared by means of liquid-phase reduction method. The size of the silver nanoparticles was 45-100 nm. On increasing concentration of sodium citrate dihydrate, the electrostatic properties decreased and, thus, the size of the silver nanoparticles is reduced. The nuclei growth rate increased on increasing concentration of ferrous sulfate dihydrate, resulting again in a size reduction of the silver nanoparticles.[15] The samples AL01 and AL02 show a rod-like morphology, whereas the samples AL03 and AL07-AL09 show a spherical morphology, and the samples AL04-AL06 show a mixed, plate-like morphology combined with spherical elements.

Table 1. Particle Size and Morphology of Silver Nanoparticles Prepared by Means of Liquid-Phase Reduction Method

Sample	$Na_3C_6H_5O_7/AgNO_3$ molar ratio	$FeSO_4/AgNO_3$ molar ratio	Particle size (nm)	Morphology
AL-01	0.1	1.0	100	Rod
AL-02	0.3	1.0	100	Rod
AL-03	0.5	1.0	100	Spherical
AL-04	0.1	0.5	–	Mix plate with spherical
AL-05	0.1	2.0	–	Mix rod with spherical
AL-06	0.1	3.0	–	Mix plate with spherical
AL-07	0.3	0.5	70-80	Spherical
AL-08	0.3	2.0	50-60	Spherical
AL-09	0.3	3.0	45-55	Spherical

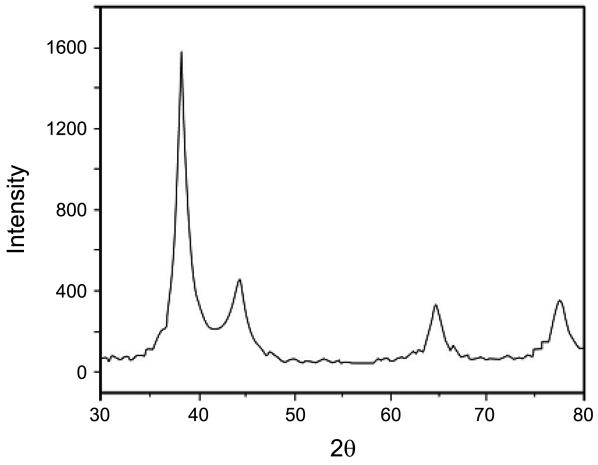

Figure 2. XRD data of silver nanoparticles prepared by liquid-phase reduction method.

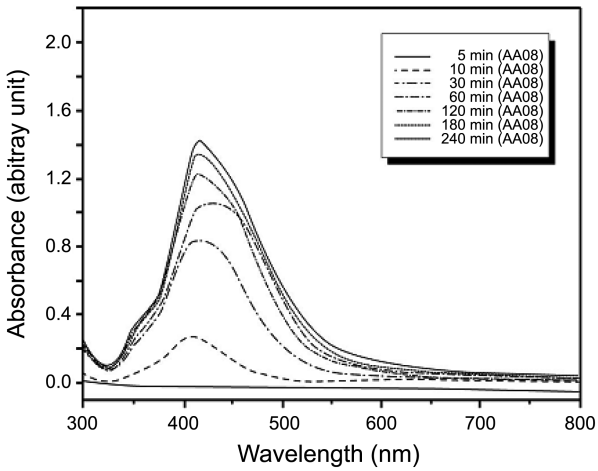

Figure 3. UV-vis spectra of silver nanoparticles prepared by alcohol-reduction method.

Figure 2 shows XRD data of silver nanoparticles prepared by liquid-phase reduction method. Four characteristic peaks appeared at 38.25°, 44.35°, 64.6°, and 77.55°, which are attributed to the (111), (200), (220), and (311) planes of silver, as shown in Figure 2(b). It can be concluded that silver nanoparticles are formed.[16]

To control the size of the silver nanoparticles, PVP K15 and K30, both with a molecular weight of M_w = 10000 g/mol and 40000 g/mol, were used for the alcohol-reduction process. The PVP K15 and K30 have a similar structure and a molecular weight that differs from that of Tween 20. Table 2 shows the size of the silver nanoparticles. The particle size was 30-100 nm. If Tween 20 was used, the AA01 and AA02 samples show a plate-like morphology. If PVP was used, the AA03-AA09 samples exhibit a spherical morphology. The dispersion state improved and the particle size decreased when PVP was used instead of Tween 20. In particular, if PVP K30 was used as polymer, the particle size decreased significantly. The particle size of silver was 40-50 nm at 1.0% PVP (AA08 sample).

Figure 3 shows UV-vis spectra of the silver nanoparticles. Generally, the UV-vis spectra of silver show a peak at about 400 nm. The peak shifted to the right when the particle size increased. As shown in Figure 3, the peak also shifted to the right and increased in intensity as the reaction progressed. This can be attributed to the fact that the formation rate of silver nanoparticles increased at the initial stage and, later,

Table 2. Particle Size and Morphology of Silver Nanoparticles Prepared by Means of Alcohol-Reduction Method

Sample	Polymer	Polymer/$AgNO_3$ molar ratio	Particle size (nm)	Morphology
AA-01	Tween 20	0.5	–	Plate
AA-02	Tween 20	1.0	60-70	Plate
AA-03	Tween 20	2.0	70-80	Spherical
AA-04	PVP (K15)	0.5	50-60	Spherical
AA-05	PVP (K15)	1.0	80-100	Spherical
AA-06	PVP (K15)	2.0	50-60	Spherical
AA-07	PVP (K30)	0.5	50	Spherical
AA-08	PVP (K30)	1.0	30-40	Spherical
AA-09	PVP (K30)	2.0	30-40	Spherical

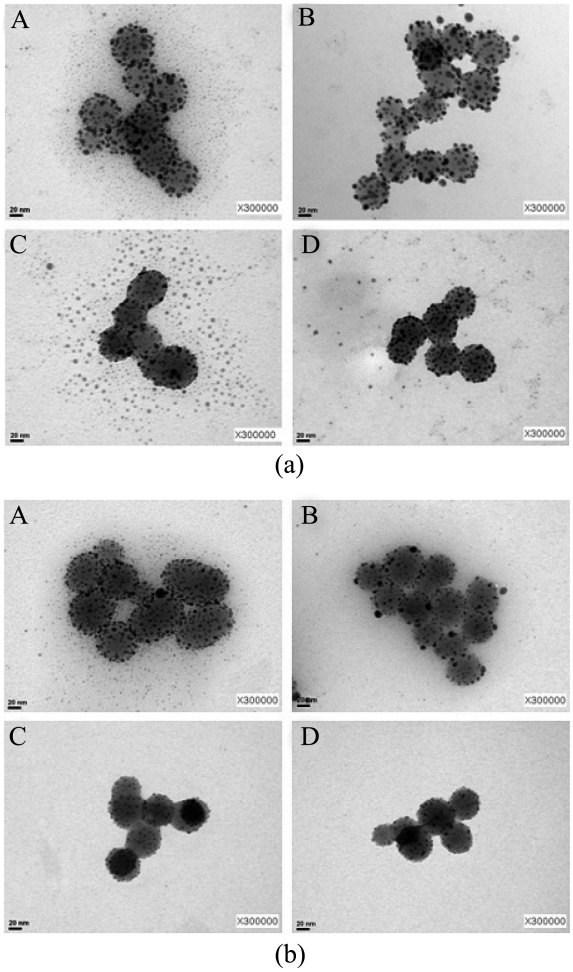

Figure 4. TEM images of silver-doped on silica treated with (a) -NH_2 group (A: M_w = 10000, B: M_w = 29000, C: M_w = 40000, D: M_w = 58000) and (b) -SH group (A: M_w = 10000, B: M_w = 29000, C: M_w = 40000, D: M_w = 58000) as a function of M_w of PVP at 0.5 wt % PVP.

the silver nanoparticles aggregated to form large particles with progressing time.[9,11]

Properties of Silver-doped Silica-complex Nanoparticles. Figure 4 shows the effect of M_w of PVP on the formation of silver-doped silica-complex nanoparticles. The average size of the nanoparticles decreased on increasing M_w of PVP. PVP monomers have imide groups that can react with metal ions and provide many active sites that improve the dispersion of silver ions and, therefore, easily dope silver nanoparticles onto silica surfaces.[14,17]

Employing PVP K15, the growth opportunities of silver nuclei increased by the presence of short polymer chains and, thus, the size of the nanoparticles increased. If M_w of PVP increased, the steric hindrance increased by the longer polymer chains, implying increased physical obstacles for the growth of silver nuclei, thereby resulting in a decreasing size of the nanoparticles. This phenomenon was observed for silver-doped silica nanoparticles prepared from silica that was treated by -NH_2 or -SH groups. In particular, if -SH group-treated silica was used, the number of doped silver particles increased and the size of the silver-doped silica nanoparticles became more homogeneous. This can be attributed to the fact that the binding energy between silver ions and -SH groups at silica surfaces is higher than that between silver ions and -NH_2 groups. Therefore, the number of silver particles doped to -SH group-treated silica surfaces was higher and more uniform, compared with -SH group-treated silica surfaces.[17]

Figure 5 shows TEM images of silver-doped silica nanoparticles treated with -NH_2 and -SH groups as a function of PVP concentration. As shown in Figure 5(a), silver nanoparticles were virtually not doped at a PVP concentration of 0.5 wt %. The size of the silver nanoparticles increased from 7-8 nm to 14-15 nm on increasing PVP concentration, while the silver nanoparticles are not doped onto the silica surfaces, but exist in solution due to the Ostwald ripening effect and steric hindrance. As shown in Figure 5(b), the silver nanoparticles are not fixed at the silica surfaces and, correspondingly, the number of particles in solution is increased. If the PVP concentration was further increased, a part of fixed silver particles forms aggregations of increased particle size. Silver nanoparticles do not exist in solution above a PVP concentration of 1.5 wt %. Above 2.5 wt %, a fraction of

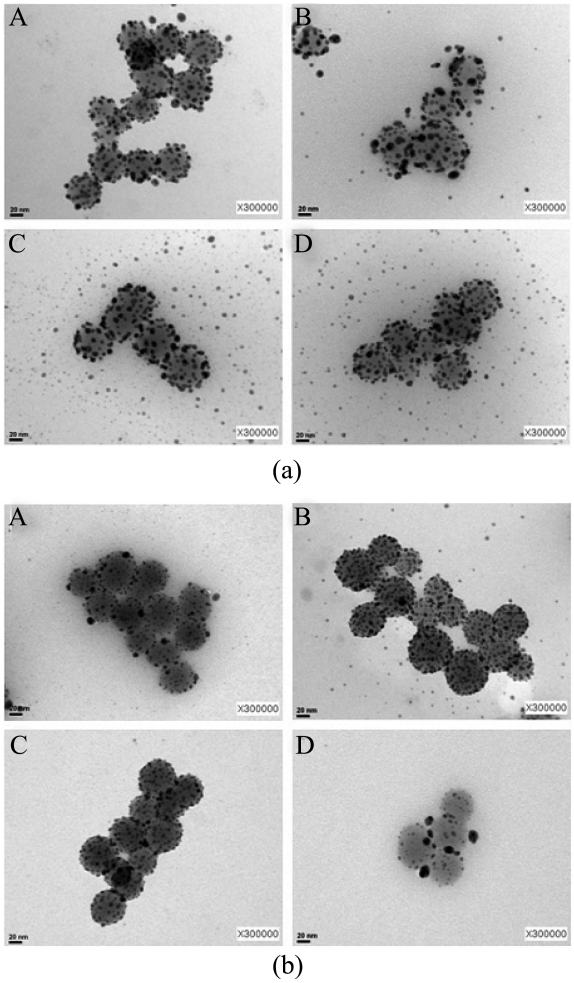

Figure 5. TEM images of silver-doped silica nanoparticles treated with (a) -NH_2 group (A: 0.5 wt % PVP, B: 1.0 wt % PVP, C: 1.5 wt % PVP, D: 2.5 wt % PVP) and (b) -SH group (A: 0.5 wt % PVP, B: 1.0 wt % PVP, C: 1.5 wt % PVP, D: 2.5 wt % PVP) as a function of PVP concentration (M_w of PVP: 29000).

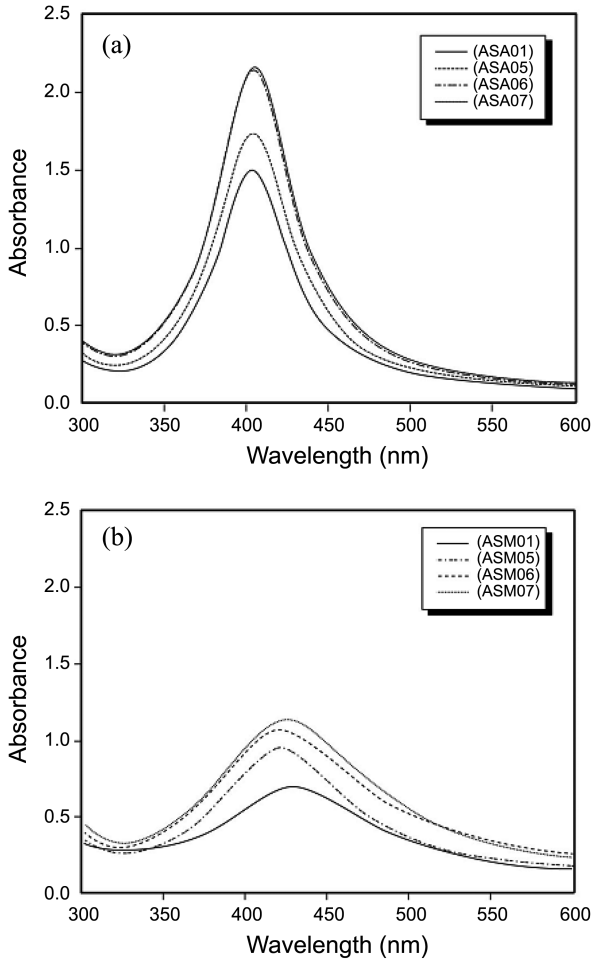

Figure 6. UV-vis absorption spectra of silver-doped silica treated with (a) -NH_2 group and (b) -SH group and different concentrations of PVP (M_w of PVP: 29000).

particles that are doped at silica surfaces aggregates and forms large particles that break away from the silica surfaces.[10,18]

Figure 6 shows UV-vis absorption spectra of silver-doped silica nanoparticles treated with -NH_2 and -SH groups as a function of PVP concentration. The absorbance in both spectra increased on increasing PVP concentration, which indicates that the size of the silver-doped silica nanoparticles increased. In case of -NH_2 groups-treated silica, the absorbance peak is not changed and, therefore, the size of the silver nanoparticles is not varied above 1.5 wt % PVP, as shown in Figure 6(a). For -SH group-treated silica, the peak at 1.5 wt % PVP is similar to that at 2.5 wt % PVP, as shown in Figure 6(b). In particular, if silica was treated with -SH groups, the nanoparticles doped at 1.0 wt % PVP formed a colloid phase and the combination of pure silver and silver-doped silica nanoparticles resulted in increased particle size on increasing PVP concentration.

Properties of the Masterbatch Chip. A silver/polyester masterbatch chip was prepared from samples AL07 (liquid-phase reduction method), AA07 and AA09 (alcohol-reduction method), and polyester, PET. The silver content of the chip was measured, and the results are shown in Table 3. The silver content of the chip prepared by alcohol reduction was higher than that prepared by liquid-phase reduction. This can be attributed to the fact that the particle size of the samples AA07 and AA09 (30-40 nm) was about half of that of sample AL07 (70-80 nm). The latter sample is dispersed uniformly and well mixed with polyester, resulting in an increased silver content.[19]

A silver-doped silica/polyester masterbatch chip was prepared by adjusting the silver content to 3000 ppm. Table 4 shows the silver content of the chip that was in the range of 2750-2900 ppm, which indicates that the silver nanoparticles are well dispersed in the silver-doped silica/polyester masterbatch chip.

Table 3. Silver Content of Silver/polyester Masterbatch Chips

Sample	Silver nanoparticles	Silver content (ppm)
AL-PM01	AL07	1115
AA-PM02	AA07	1205
AA-PM03	AA09	1315

Note: AL-PM: Silver/polyester masterbatch chip prepared by liquid-phase reduction method; AA-PM: Silver/polyester masterbatch chip prepared by alcohol-reduction method.

Table 4. Silver Content of Silver-doped Silica/polyester Masterbatch Chips

Sample	Silver-silica composite	Silver content (ppm)
ASA-PM01	ASA02	2750
ASA-PM02	ASA05	2800
ASA-PM03	ASA06	2800
ASM-PM01	ASM02	2900
ASM-PM02	ASM04	2850
ASM-PM03	ASM06	2900

Note: ASA-PM: Silver-silica-APTMS/polyester masterbatch chip; ASM-PM: Silver-silica-MPTMS/polyester masterbatch chip.

Table 5. Antibacterial Properties of Silver/polyester and Silver-doped Silica/polyester Masterbatch Chips

Sample	Bacterial reduction ratio (%)	
	S. aureus	*E. coli*
AL-PM01	99.9	99.9
AA-PM02	99.9	99.9
AA-PM03	99.9	99.9
ASA-PM03 (1%)	29.9	55.2
ASA-PM03 (3%)	80.5	92.3
ASA-PM03 (5%)	99.9	99.9
ASM-PM03 (1%)	58.1	63.5
ASM-PM03 (3%)	99.9	98.7
ASM-PM03 (5%)	99.9	99.9

Antibacterial Properties. The antibacterial properties of the silver/polyester masterbatch chips were evaluated by using *E. coli* and *S. aureus*, and the results are shown in Table 5. The bacterial reduction ratio of the chips prepared by either liquid-phase or alcohol-reduction was 99.8-99.9%, which implies a high antimicrobial activity.[20-23]

The antibacterial properties were investigated by varying the silver content of the silver-doped silica/polyester masterbatch chip, and the results are also shown in Table 5. If the chip was treated with -NH_2, the bacterial reduction ratio shows low values at silver concentrations of 1-3 wt %, but it increased to 99.9% at 5 wt % of nanoparticles. If the chip was treated with -SH, the bacterial reduction ratios of the chips at 3 wt % and 5 wt % silver were 98.7% and 99.9%, respectively, which evidences a high antimicrobial activity. Based on the above results, to give an optimal antimicrobial activity to spun polyester tissue, the content of silver-doped silica-complex particles in the masterbatch chip should reach 5 wt %.[24-27]

Conclusions

Silver nanoparticles and silver-doped silica-complex nanoparticles were prepared, and the formation, structure, morphology, and size of the nanoparticles were studied. The sizes of silver nanoparticles prepared by liquid-phase and alcohol reduction were 45-100 nm and 30-100 nm, respectively. The average size of silver-doped silica nanoparticles treated with amino groups increased on increasing PVP concentration, but it does not affect the size of silver-doped silica nanoparticles treated with mercapto groups. The silver content of a silver/polyester masterbatch chip prepared by the alcohol-reduction method was higher than that prepared by the liquid-phase reduction method. The antibacterial tests indicated that the optimal content of silver-doped silica-complex particles in the masterbatch chip was 5 wt %. These encouraging results indicate that silver-doped silica-complex nanoparticles may have a wide range of applications in antibacterial materials.

Acknowledgments. (1) This research was supported by a

grant from the Fundamental R&D Program for Core Technology of Materials funded by the Ministry of Knowledge Economy, Korea. (2) This research was financially supported by National Research Foundation of Korea (NRF) through the Human Resource Training Project for Regional Innovation (No. 2012-10-A-04-046-13-010100).

References

1. Tang, B.; Wang, J.; Xu, S.; Afrin, T.; Xu, W.; Sun, L.; Wang, X. *J. Colloid Interf. Sci.* **2011**, *356*, 513.
2. Jiang, S. Q.; Newton, E.; C. Yuen, W. M. C.; Kan, W. *J. Appl. Polym. Sci*. **2005**, *96*, 919.
3. Pasricha, A.; Jangra, S. L.; Singh, N.; Dilbaghi, N.; Sood, K. N.; Arora, K.; Pasricha, R. *J. Environ. Sci*. **2012**, *24*, 852.
4. Jung, W. K.; Kim, S. H.; Koo, H. C.; Shin, S.; Kim, J. M.; Park, Y. K.; Hwang, S. Y.; Yang, H.; Park, Y. H. *Mycoses* **2007**, *50*, 265.
5. Kramar, A.; Prysiazhnyi, V.; Dojčinović, B.; Mihajlovski, K.; Obradović, B. M.; Kuraica, M. M.; Kostić, M. *Surf. Coat. Tech*. **2013**, *234*, 92.
6. Sataev, M. S.; Koshkarbaeva, S. T.; Tleuova, A. B.; Perni, S.; Aidarova, S. B.; Prokopovich, P. *Colloid Surface A* **2014**, *442*, 146.
7. Babu, K. F.; Dhandapani, P.; Maruthamuthu, S.; Kulandainathan, M. A. *Carbohyd. Polym*. **2012**, *90*, 1557.
8. Messaoud, M.; Chadeau, E.; Brunon, C.; Ballet, T.; Rappenne, L.; Roussel, F.; Leonard, D.; Oulahal, N.; Langlet, M. *J. Photoch. Photobio. A* **2010**, *215*, 147.
9. Yang, N.; Li, W. H. *Ind. Crop Product* **2013**, *48*, 81.
10. El-Rafie, M. H.; Shaheen, Th. I.; Mohamed, A. A.; Hebeish, A. *Carbohyd. Polym*. **2012**, *90*, 915.
11. El-Rafie, M. H.; Mohamed, A. A.; Shaheen, Th. I.; Hebeish, A. *Carbohyd. Polym*. **2010**, *80*, 779.
12. Tang, B.; Wang, J.; Xu, S.; Afrin, T.; Tao, J.; Xu, W.; Sun, L.; Wang, X. *Chem. Eng. J*. **2012**, 1*85-186*, 366.
13. Montazer, M.; Shamei, A.; Alimohammadi, F. *Prog. Org. Coat*. **2012**, *75*, 379.
14. Tarimala, S.; Kothari, N.; Abidi, N.; Hequet, E.; Fralick, J.; Dai, L. L. *J. Appl. Polym. Sci*. **2006**, *101*, 2938.
15. Vu, N. K.; Zille, A.; Oliveira, F. R.; Carneiro, N.; Souto, A. P. *Plasma Process. Polym*. **2013**, *10*, 285.
16. Lu, Y.; Liang, Q.; Xue, L. *Surf. Coat. Tech*. **2012**, *206*, 3639.
17. Yang, F. C.; Wu, K. H.; Huang, J. W.; Horng, D. N.; Liang, C. F.; Hu, M. K. *Mater. Sci. Eng. C* **2012**, *32*, 1062.
18. Patil, K.; Wang, X.; Lin, T. *Powder Technol*. **2013**, *245*, 40.
19. Park, M. R.; Kim, H. Y.; Jin, F. L.; Park, S. J. *J. Ind. Eng. Chem.* **2014**, *20*, 179.
20. Radetić, M.; Ilić, V.; Vodnik, V.; Dimitrijević, S.; Jovančić, P.; Šaponjic, Z.; Nedeljković, J. M. *Polym. Adv. Technol*. **2008**, *19*, 1816.
21. Shin, H. K.; Chung, Y. S.; Park, M.; Kim, H. Y.; Jin, F. L.; Park, S. J. *J. Ind. Eng. Chem.* **2014**, *20*, 1476.
22. Yun, H.; Kim, J. D.; Choi, H. C.; Lee, C. W. *Bull. Korean Chem. Soc*. **2013**, *34*, 3261.
23. Shin, H. K.; Chung, Y. S.; Park, M.; Kim, H. Y.; Jin, F. L.; Park, S. J. *Macromol. Res.* **2013**, *21*, 1241.
24. Ilić, V.; Šaponjić, Z.; Vodnik, V.; Potkonjak, B.; Jovančić, P.; Nedeljković, J.; Radetic, M. *Carbohyd. Polym*. **2009**, *78*, 564.
25. Yoo, Y. C.; Kim, H. Y.; Jin, F. L.; Park, S. J. *Bull. Korean Chem. Soc*. **2012**, *33*, 4137.
26. Yue, L.; Wang, Q.; Zhang, X.; Wang, Z.; Xia, W.; Dong, Y. *Bull. Korean Chem. Soc*. **2011**, *32*, 2607.
27. Shin, H. K.; Chung, Y. S.; Park, M.; Kim, H. Y.; Jin, F. L.; Park, S. J. *Bull. Korean Chem. Soc*. **2013**, *34*, 2441.